Assignment of the excess absorption underlying the Schumann–Runge bands of molecular oxygen

B. R. Lewis, S. T. Gibson, and E. H. Roberts

Articles you may be interested in

The Huggins band of ozone: Unambiguous electronic and vibrational assignment
J. Chem. Phys. 120, 6811 (2004); 10.1063/1.1711589

Ab initio calculation of predissociation linewidths in the Schumann–Runge bands of the oxygen molecule
J. Chem. Phys. 114, 10396 (2001); 10.1063/1.1370529

Time-dependent quantum mechanical study of photodissociation of molecular oxygen in the Schumann–Runge continuum
J. Chem. Phys. 112, 1255 (2000); 10.1063/1.480657

A comparative high-resolution study of predissociation linewidths in the Schumann-Runge bands of O 2
J. Chem. Phys. 109, 3856 (1998); 10.1063/1.476986

Fine-structure dependence of predissociation linewidth in the Schumann–Runge bands of molecular oxygen
J. Chem. Phys. 100, 7012 (1994); 10.1063/1.466902

Assignment of the excess absorption underlying the Schumann−Runge bands of molecular oxygen

B. R. Lewis, S. T. Gibson, and E. H. Roberts
Research School of Physical Sciences and Engineering, The Australian National University, Canberra, ACT 0200, Australia

A long-standing problem, pertaining to the origin of the excess absorption found experimentally to underlie the high-vibrational Schumann–Runge bands of molecular oxygen, is resolved. Through new calculations, with parameter sets based on recently obtained experimental information, it is shown that the excess absorption arises from transitions into the lowest valence states of $^3\Pi_u$ and $^3\Pi_g$ symmetry. © *2001 American Institute of Physics.* [DOI: 10.1063/1.1379335]

I. INTRODUCTION

Photoabsorption of solar vacuum-ultraviolet (VUV) radiation in the Schumann–Runge (SR) region of the O_2 spectrum, leading to photodissociation, plays an important role in the photochemistry of the terrestrial atmosphere. In particular, predissociation in the SR bands, $B\,^3\Sigma_u^-\leftarrow X\,^3\Sigma_g^-(v,0)$ (1750–2050 Å), provides significant production of odd oxygen in the stratosphere and the dominant mesospheric source. There are other contributors to O_2 opacity in the area of the SR bands which become significant in the regions of weak absorption between rovibrational SR lines, corresponding to the deeper penetration of solar VUV radiation into the atmosphere. First, the forbidden Herzberg I, II, and III continua, $A\,^3\Sigma_u^+\leftarrow X\,^3\Sigma_g^-$, $c\,^1\Sigma_u^-\leftarrow X\,^3\Sigma_g^-$, and $A'\,^3\Delta_u\leftarrow X\,^3\Sigma_g^-$, respectively, the latter pressure dependent,[1] together provide significant absorption at the longer wavelengths.[2] Second, temperature-dependent photoabsorption from rovibrationally excited ground-state levels into the continuum of the B state is important at the shorter wavelengths.[3] Finally, there appears to be an ''excess absorption'' which increases towards the shorter wavelengths,[4] but is yet to be explained satisfactorily. It is the origin of this excess absorption which is the principal subject of this communication.

Experimental measurements of the absorption underlying the SR bands have been reviewed by Lewis *et al.*[4] The only detailed measurements in the 1750–1900 Å range, of principal interest in this work, are due to Ogawa[5] and Lewis *et al.*[4] The notion of an excess absorption was introduced[6] to accommodate differences between computational models of the SR system and the experimental measurements, although Blake[7] maintained that such a procedure was unnecessary. Imputed values of the excess absorption are critically dependent on the accuracy of the SR-band wing correction. Most SR models have assumed a Lorentzian line shape for the component due to predissociation. Using such a model, Lewis *et al.*[4] deduced an excess cross section which rose from a small value at 1900 Å, to $1-2\times10^{-21}$ cm^2 at 1760 Å. Very recently, these values have been revised,[8] downwards at the shorter wavelengths (e.g., from 5.5 to 1.3 $\times10^{-22}$ cm^2 at 1780 Å), through the employment of a coupled-channel (CC) model of the SR absorption which al-

lowed for the non-Lorentzian line shapes caused by quantum interference effects.[9]

It was suggested initially that electric-dipole absorption into the repulsive $1\,^3\Pi_u$ state was the principal source of the excess absorption.[5,6] However, *ab initio* calculations of the $1\,^3\Pi_u-X$ photoabsorption yielded negligible cross sections ($\lesssim10^{-23}$ cm^2) in the upper SR-band region.[10,11] This led to the suggestion that magnetic-dipole absorption into the $1\,^3\Pi_g$ state was responsible for the excess absorption.[4] However, calculations of the $^3\Pi_g-X$ cross section showed that there was little possibility of this, values of $\lesssim10^{-23}$ cm^2 again being obtained.[12] Thus, despite a decrease over the years in the estimated magnitude of the excess absorption, current theoretical models still underpredict experiment by at least an order of magnitude. In the following sections, we present revised semiempirical models of the $^3\Pi_{u,g}-X$ photoabsorptions, based on significant new experimental information, in an attempt to resolve this discrepancy.

II. CALCULATIONS

A. The $^3\Pi_u\leftarrow X\,^3\Sigma_g^-$ transition

The model adiabatic $1\,^3\Pi_u$ potential-energy curve (PEC) and electronic transition moment (ETM) employed in the present calculation of the $1\,^3\Pi_u-X$ photodissociation cross section are shown in Figs. 1(a) and 1(b), respectively. For internuclear distances $R\geqslant1.3$ Å, the $1\,^3\Pi_u$ PEC was derived from the multireference configuration–interaction plus Davidson correction (MRCI+Q) *ab initio* PEC of Partridge *et al.*,[13] shifted up in energy to the experimental O(^3P) +O(^3P) dissociation limit, shifted to shorter R by 4 mÅ, in order to reproduce the B-state crossing point $R_x=1.454\pm0.002$ Å known from a study of the B-state predissociation,[14] and expanded about R_x by 1.7%, in order to join smoothly onto the short-R part of the PEC described below. These small adjustments are similar in magnitude and sense to those required to force agreement between MRCI+Q and experimental PECs for the $A\,^3\Sigma_u^+$ and $A'\,^3\Delta_u$ states of O_2,[2] and the resultant slope of the model PEC at R_x agrees with that found experimentally[14] to within the corresponding uncertainty. For $R<1.3$ Å, we adopted the $1\,^3\Pi_u$ adiabatic PEC of Lewis *et al.*,[15] obtained from a diabatic CC
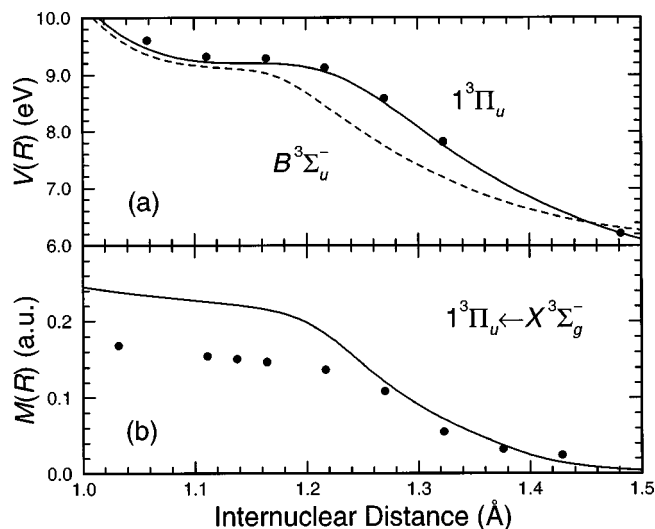
FIG. 1. Comparison between adiabatic model parameters used for the $1\,^3\Pi_u-X$ calculations and *ab initio* values. (a) PECs $V(R)$, referred to the minimum in the $X\,^3\Sigma_g^-$ PEC (not shown). Solid curve: Model $1\,^3\Pi_u$ PEC. Filled circles: *Ab initio* $1\,^3\Pi_u$ PEC (Ref. 13). Dashed curve: $B\,^3\Sigma_u^-$ PEC. (b) ETMs $M(R)$. Solid curve: Model $1\,^3\Pi_u-X$ ETM. Solid circles: *Ab initio* ETM (Ref. 19).
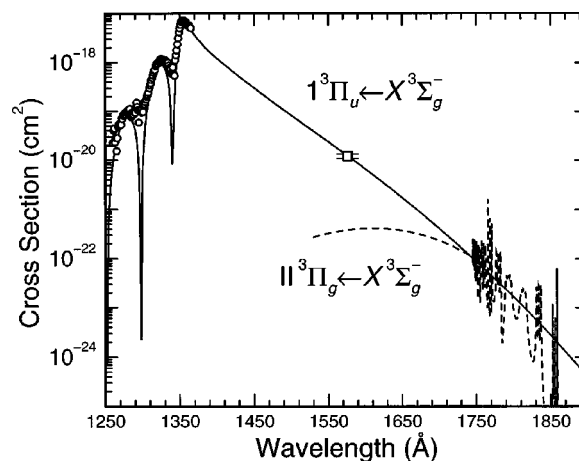

FIG. 2. $^3\Pi_{u,g}-X$ photodissociation cross sections. Solid curve: Model $1\,^3\Pi_u-X$ calculation. Open circles: $1\,^3\Pi_u-X$ cross section from experimental fluorescence-excitation spectrum (Ref. 20). Open square: $1\,^3\Pi_u-X$ cross section from experimental photofragment spectrum (Ref. 17). Dashed curve: Model $\mathrm{II}\,^3\Pi_g-X$ calculation.

treatment of the strong $^3\Pi_u$ Rydberg-valence interaction, involving a least-squares fit to all available experimental information on the $1\,^3\Pi_u$ and $F\,^3\Pi_u$ states. In Fig. 1(a), it is seen that our adopted PEC is in good agreement overall with the MRCI+Q PEC,[13] which has been supplemented by extra points calculated in the region of the Rydberg-valence crossing.[16]

The model $1\,^3\Pi_u-X$ ETM was derived using the CC method of Lewis *et al.*,[15] whereby diabatic Rydberg and valence ETMs with linear R dependences were adjusted to optimize agreement with experimental intensities for $1\,^3\Pi_u-X$ and $F-X$ spectral features. However, our ETM differs significantly for $R>1.25$ Å from that of Lewis *et al.*,[15] since we have included a $1\,^3\Pi_u-X$ photodissociation cross section of $(1.20\pm0.12)\times10^{-20}$ cm^2 at 1576 Å, deduced from recent photofragment spectra,[17] in the optimization procedure. This value follows from an experimental 0.198% branching ratio for $1\,^3\Pi_u$ photodissociation[17] and a total SR cross section of 6.06×10^{-18} cm^2.[18] For the insensitive region $R>1.4$ Å, the model ETM has been extrapolated exponentially to zero at large R. In Fig. 1(b), the model ETM is seen to be in reasonable agreement with a recent *ab initio* calculation[19] for $R>1.25$ Å, but to be significantly larger in the Rydberg region at shorter R.

The $1\,^3\Pi_u-X$ photodissociation cross section calculated using the model PEC and ETM, together with a Rydberg–Klein–Rees PEC for the X state, is shown in Fig. 2. The rotationless calculations were performed using the expression[11]

$$\sigma(\lambda)=\frac{2.45\times10^{-15}}{\lambda}|\langle\chi_E(R)|M(R)|\chi_0(R)\rangle|^2, \quad (1)$$

where the cross section $\sigma(\lambda)$ is in cm^2, the transition wavelength λ is in Å, and the transition matrix elements are in a.u. Radial wavefunctions, $\chi_0(R)$ for the discrete initial state

$X(v=0)$, and $\chi_E(R)$ for the continuous final state $1\,^3\Pi_u$, the latter energy normalized, were determined by numerical solution of appropriate Schrödinger equations. The computed cross section in Fig. 2 is in excellent agreement with that derived from fluorescence-excitation spectra in the region of the diffuse structure between 1270 and 1370 Å ,[20] and also with the single point at 1576 Å from photofragment spectra,[17] the only experimentally based data available. However, the computed cross section is significantly larger than the results of previous calculations,[10,11,21] particularly at the longer wavelengths, and by at least an order of magnitude at 1576 Å.

B. The $^3\Pi_g\leftarrow X\,^3\Sigma_g^-$ transition

In contrast to the $^3\Pi_u$ states, the $^3\Pi_g$ states of O$_2$ behave *diabatically*, with only relatively weak couplings between the I and II $^3\Pi_g$ valence states[22] and the II $^3\Pi_g$ and $C\,^3\Pi_g$ Rydberg state.[23] Therefore, in contrast to previous computational methods which employed a single adiabatic PEC for the $1\,^3\Pi_g$ state, we implement a CC model involving the two diabatic valence states, coupled with an interaction $H^{\mathrm{el}}=500$ cm^{-1},[23] in order to compute the cross section for the magnetic-dipole transition to the predissociated II $^3\Pi_g$ state. Henceforth, we will use the diabatic notation II $^3\Pi_g-X$ to describe the CC cross section.

Our model $^3\Pi_g$ diabatic PECs, shown in Fig. 3, are similar to those of Roberts *et al.*,[24] designed to reproduce the II $^3\Pi_g(v=0)$ energy and rotational constant determined experimentally following their very recent observation of the II $^3\Pi_g-X$ magnetic-dipole transition. In addition, however, we require that the II $^3\Pi_g$ valence PEC cross the $C\,^3\Pi_g$ Rydberg PEC with the crossing point and slope necessary to reproduce the experimental pattern of predissociation for the C-state vibrational levels.[23] The resultant II $^3\Pi_g$ PEC was obtained from a diabatic PEC deduced from the MRCI+Q PECs of Partridge,[16] also shown in Fig. 3, following a shift of 6 mÅ to shorter R, a decrease in well depth by 3%, and an expansion about R_e by 1.4%. The model I $^3\Pi_g$ PEC was
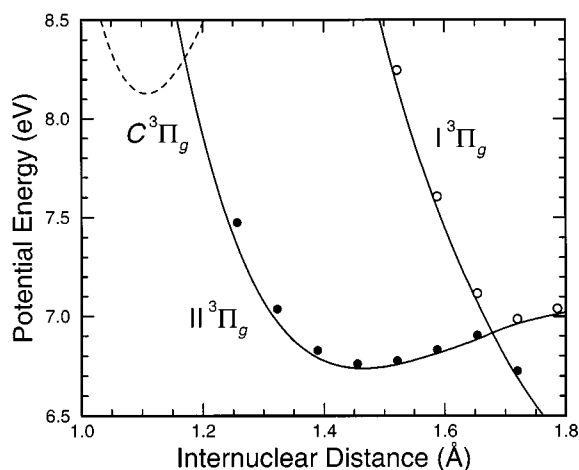
FIG. 3. Comparison between model diabatic valence PECs used for the II $^3\Pi_g$–X calculations (solid curves) and the MRCI+Q adiabatic PECs of Ref. 16, referred to the O(^3P)+O(^3P) dissociation limit (circles). The Rydberg $C\,^3\Pi_g$ PEC is also shown (dashed curve).

FIG. 4. Excess absorption underlying the upper SR-band region. Open circles: Non-SR cross section derived from the $T\approx 80$ K measurements of Ref. 4 by Lewis et al. (Ref. 8). Solid curve: Sum of present rotationless 1 $^3\Pi_u$–X and II $^3\Pi_g$–X cross sections and a Herzberg continuum computed according to the method of Buijsse et al. (Ref. 2). Locations of the II $^3\Pi_g$ $-X(v,0)$ bands are also shown.

obtained from the corresponding MRCI+Q-derived diabatic PEC assuming a similar shift in R of -6 mÅ.

The II $^3\Pi_g\leftarrow X$ cross section was determined using a multichannel form of Eq. (1), described by Roberts et al.,[24] in which the excited-state wave functions are the solutions of a CC Schrödinger equation, and the only nonzero element of the TM vector is the diabatic magnetic-dipole TM for the II $^3\Pi_g$–X transition $|M(R)|=\alpha|\langle L_+\rangle|/2$,[12] where α is the fine-structure constant and $\langle L_+\rangle$ is the expectation value of the angular-momentum raising operator between the X and II $^3\Pi_g$ states. Here, we take $|\langle L_+\rangle|=0.9$ a.u., independent of R, this value being necessary to reproduce the experimental oscillator strength for the II $^3\Pi_g$–$X(0,0)$ band,[24] and in reasonable agreement with the ab initio value 1.16 a.u. (calculated at $R=2.28$ a.u.).[25] The resultant model rotationless II $^3\Pi_g$–X photodissociation cross section, including triplet structure, and also shown in Fig. 2, peaks at $\sim 4\times10^{-22}$ cm^2 near 1610 Å , corresponding to a vertical excitation energy of 7.70 eV, in reasonable agreement with the 7.65 ± 0.03 eV determined from a decomposition of electron energy-loss spectra.[26] The model cross section is an order of magnitude lower than the estimate of Lewis et al.,[4] but an order of magnitude higher than the calculation of Friedman and Dalgarno.[12] In the continuum near the B-state dissociation limit (~ 1750 Å), both the II $^3\Pi_g$–X and 1 $^3\Pi_u$–X cross sections have similar magnitudes ($\sim 10^{-22}$ cm^2).

III. DISCUSSION AND CONCLUSIONS

The sum of the model rotationless 1 $^3\Pi_u$–X, II $^3\Pi_g$–X, and Herzberg I, II, and III cross sections[2] is compared in Fig. 4 with the non-SR excess cross section[8] deduced from experiment.[4] The model cross section $\approx 2\times10^{-22}$ cm^2 near 1750 Å and is in reasonable overall agreement with the measurements. Thus, previous serious discrepancies between experimental and computed excess cross sections have been resolved: transitions into both $^3\Pi_u$ and $^3\Pi_g$ states make significant contributions to the excess absorption. This resolution has required advances on three fronts: first, allowance
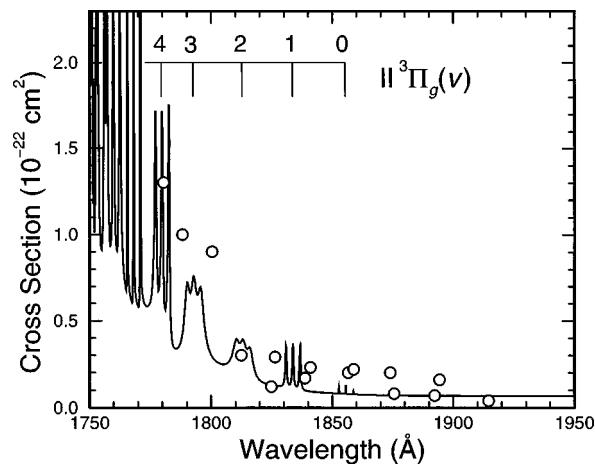
for non-Lorentzian line shapes in the SR wing corrections;[8] second, the elucidation of the 1 $^3\Pi_u$–X cross section provided by the photofragment spectrum of Lin et al.;[17] and third, the observation of the magnetic-dipole transition II $^3\Pi_g$–$X(0,0)$.[24] The higher cross sections of this work, compared with previous calculations, result principally from the use of improved PECs. Further confirmation of the model might be provided by the future observation of the higher bands of the magnetic-dipole transition in the absorption underlying the SR bands. Finally, while it seems clear that the $^3\Pi_{u,g}$–X excess absorption can be detected experimentally, its significance in atmospheric photochemical models may be marginal, considering that it constitutes only $\sim 20\%$ of the absorption in the deepest windows between SR lines in the $\lambda\lesssim 1800$ Å region.

[1] A. J. Blake and D. G. McCoy, J. Quant. Spectrosc. Radiat. Transf. **38**, 113 (1987).
[2] B. Buijsse, W. J. van der Zande, A. T. J. B. Eppink, D. H. Parker, B. R. Lewis, and S. T. Gibson, J. Chem. Phys. **108**, 7229 (1998).
[3] S. T. Gibson, B. R. Lewis, K. G. H. Baldwin, and J. H. Carver, J. Chem. Phys. **94**, 1060 (1991).
[4] B. R. Lewis, L. Berzins, J. H. Carver, S. T. Gibson, and D. G. McCoy, J. Quant. Spectrosc. Radiat. Transf. **34**, 405 (1985).
[5] M. Ogawa, J. Chem. Phys. **54**, 2550 (1971).
[6] T. M. Fang, S. C. Wofsy, and A. Dalgarno, Planet Space Sci. **22**, 413 (1974).
[7] A. J. Blake, J. Geophys. Res. **84**, 3272 (1979).
[8] B. R. Lewis, S. T. Gibson, F. T. Hawes, and L. W. Torop, Phys. Chem. Earth C **26**, 519 (2001).
[9] B. R. Lewis, S. T. Gibson, L. W. Torop, and D. G. McCoy, Geophys. Res. Lett. **25**, 2457 (1998).
[10] S. L. Guberman and A. Dalgarno, J. Geophys. Res. **84**, 4437 (1979).
[11] A. C. Allison, S. L. Guberman, and A. Dalgarno, J. Geophys. Res. **87**, 923 (1982).

[12] R. S. Friedman and A. Dalgarno, J. Quant. Spectrosc. Radiat. Transf. **42**, 137 (1989).

[13] H. Partridge, C. W. Bauschlicher, Jr., S. R. Langhoff, and P. R. Taylor, J. Chem. Phys. **95**, 8292 (1991).

[14] B. R. Lewis, S. T. Gibson, and P. M. Dooley, J. Chem. Phys. **100**, 7012 (1994).

[15] B. R. Lewis, J. P. England, S. T. Gibson, M. J. Brunger, and M. Allan, Phys. Rev. A **63**, 022707 (2001).

[16] H. Partridge (private communication).

[17] J. J. Lin, D. W. Hwang, Y. T. Lee, and X. Yang, J. Chem. Phys. **109**, 1758 (1998).

[18] S. T. Gibson, H. P. F. Gies, A. J. Blake, D. G. McCoy, and P. J. Rogers, J. Quant. Spectrosc. Radiat. Transf. **30**, 385 (1983).

[19] D. Spelsberg and W. Meyer, J. Chem. Phys. **109**, 9802 (1998).

[20] S. T. Gibson and B. R. Lewis, J. Electron Spectrosc. Relat. Phenom. **80**, 9 (1996).

[21] J. F. Babb, Y. Sun, M. J. Jamieson, A. Dalgarno, and A. C. Allison, J. Quant. Spectrosc. Radiat. Transf. **50**, 579 (1993).

[22] W. J. van der Zande, W. Koot, and J. Los, J. Chem. Phys. **91**, 4597 (1989).

[23] J. S. Morrill, M. L. Ginter, B. R. Lewis, and S. T. Gibson, J. Chem. Phys. **111**, 173 (1999).

[24] E. H. Roberts, K. L. Nixon, C. J. Dedman, S. T. Gibson, and B. R. Lewis (unpublished).

[25] R. Klotz, C. M. Marian, S. D. Peyerimhoff, B. A. Hess, and R. J. Buenker, Chem. Phys. **89**, 223 (1984).

[26] T. W. Shyn, C. J. Sweeney, A. Grafe, and W. E. Sharp, Phys. Rev. A **50**, 4794 (1994).